Improving the signal uniformity at 400 MHz: sequential multi-channel excitation with intermediate active shims

V. Taracila[1], L. S. Petropoulos[1,2], T. P. Eagan[1], R. W. Brown[1]

[1]Department of Physics, Case Western Reserve University, Cleveland, OH, United States, [2]Hitachi Medical Systems, Twinsburg, OH, United States

Introduction

The advantages offered by increased signal-to-noise (SNR) and improved resolution in ultra-high-field MRI systems may be offset by severe RF field inhomogeneities. At 400 MHz, the wavelength of the EM waves is only λ_0=75 cm in the air, while in the human body (ε=58, σ=0.4-1.5 S/m) it reduces to $\lambda = \lambda_0/\sqrt{\varepsilon} = 9.8$ cm . RF field inhomogeneities become severe for volumetric type coils like a birdcage coil where wave interference resulting in bright spots have been observed at phantoms and humans. The MR community often refers to these RF nonuniformities as "dielectric resonance" effects[1]. Various attempts over the past few years have been made, with varying success, to modify the current distributions on volumetric coils [2],[3],[4] in order to improve the RF field homogeneity inside the desired imaging region.

We present an alternative way to improve signal uniformity of a birdcage by using multi-channel excitations in one combined RF pulse to decrease the scanning time. To build up a uniform transverse magnetization constructively for the entire sample cross-section and at any flip angle, it is necessary to utilize additional small fields, referred to here as "active" shims (such shims are not driven at the Larmor frequency), interspersed with the RF pulses. Due to topological spin singularities associated with the channels n=2,3,… , the uniformity of the signal can only be achieved locally and not over the entire sample cross-section.

Materials and Methods

For the electromagnetic field computation the 2D full wave solution [5] of the shielded birdcage coil, with respective radii 14.6 cm and 17.6 cm, surrounding a concentric cylindrical phantom with radius of 9.25 cm, electric permittivity 58 and conductivity 0.7. Assuming the continuity of the transverse and normal components of the magnetic field at all boundaries, we find the components of the magnetic field $B_{x,n}(r,\varphi)$ and $B_{y,n}(r,\varphi)$ inside and outside the sample. Since only clockwise polarized components of the field tip spins into transverse plane, the effective field components of the original EM solution are $B^+_{x,n}(r,\varphi)$ and $B^+_{y,n}(r,\varphi)$ represent effective tipping components in the rotating reference frame. The

$$B^+_{x,n}(r,\varphi) = \frac{1}{2}\left(\mathrm{Re}[B_{x,n}(r,\varphi)] - \mathrm{Im}[B_{y,n}(r,\varphi)]\right), \quad B^+_{y,n}(r,\varphi) = \frac{1}{2}\left(\mathrm{Im}[B_{x,n}(r,\varphi)] + \mathrm{Re}[B_{y,n}(r,\varphi)]\right).$$

phase map of the magnetic field everywhere across the sample is then constructed as $\alpha_n(r,\varphi) = \arctan\left[B^+_{n,y}(r,\varphi)/B^+_{n,x}(r,\varphi)\right]$.

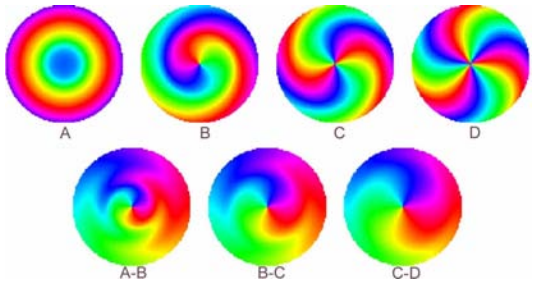

Fig. 1.Upper row: Phase map of cos$n\varphi$ RF channels: A) n=1; B) n=2; C) n=3; D) n=4; Lower row: Phase differences between

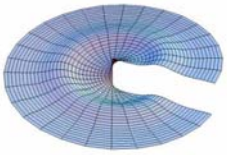

Fig. 2. Cylindrical plot of additional magnetic field

Each RF channel is characterized by its own phase map (Fig.1). In the upper row of Fig. 1 are corresponding phase map phases for cosφ, cos2φ, cos3φ and cos4φ RF modes on a birdcage-like coil. Applying the Larmor relation $\omega = \gamma B_z$ to the lower row of Fig.1 the 2D vector field of the differences of $\cos n\varphi$ may be related to a single component of the additional magnetic fields via the form $\Delta B_{z,n\to n+1}(r,\varphi) = \left[\alpha_{n+1}(r,\varphi) - \alpha_n(r,\varphi)\right]/(\gamma\tau_{n,n+1})$, where $\tau_{1,2}$, $\tau_{2,3}$, $\tau_{3,4}$ are the time durations of the additional magnetic fields $\Delta B_{z,1\to 2}(r,\varphi)$, $\Delta B_{z,2\to 3}(r,\varphi)$ and $\Delta B_{z,3\to 4}(r,\varphi)$ needed to correct the phase , respectively. Fig. 2 represents the plot of the desired magnetic field $\Delta B_{z,1\to 2}(r,\varphi)$ needed to adjust the phase of the image between each scan. However, due to the topological spin singularity of the $\cos 2\varphi$ term of the RF channel there is a $2\pi/(\gamma\tau_{12})$ gap in the field. Assuming a $\tau \approx 1$ ms pulse, the additional magnetic field required will be of the order $\Delta B \approx 20\mu$T which is on the same order of magnitude as actively controlled resistive main magnetic field shims. Figure 3 illustrates a possible scenario for combining sequences of RF pulses and active shims in order to get a more uniform localized signal.

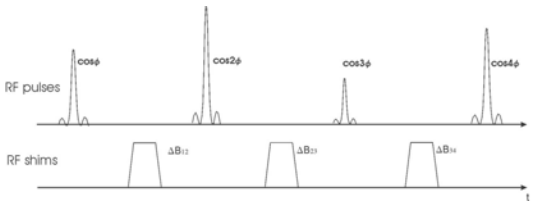

Fig. 3. Sequential application of RF

Results and Discussion

Numerical evaluation of the resulting transverse magnetization is made utilizing a set-up illustrated in Figure 3 and optimizing the contribution of each phase map with the appropriate weighting factors. The signal nonuniformity inside the phantom has been improved from 50% (a typical birdcage coil result at 400MHz) down to 7 %, by using all the higher order terms, in the region of the phantom that excludes the field singularities. Employing the sequence of pulses and active shims from Figure 3 and solving numerically the Bloch equation [6] for this sequence, we find the result shown in Fig. 4. With this technique it is thus possible to achieve locally a very uniformly transverse magnetization at 400 MHz, utilizing a sequential RF pulse method interleaved with application of the appropriate active shims. However, this technique cannot correct globally such nonuniformities at 400 MHz due to the spin singularities inside the phantom.

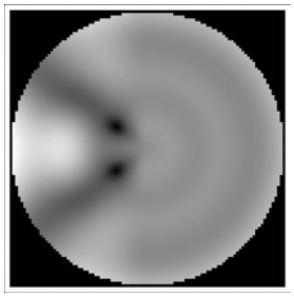

Fig. 4. Resulting image of the combined RF pulse, assisted by RF shims

Acknowledgment

The authors would like to acknowledge the Ohio Third Frontier Program for support. We thank Dr. W. Edelstein for helpful discussions.

References

[1] J. Tropp, Journal of Magnetic Resonance, 167 (2004) 12-24;
[2] V. Taracila et al. , ISMRM 2005, Miami;
[3] T. Ibrahim, ISMRM 2005, Miami;
[4] T. Vaughan et al., ISMRM 2005, Miami;
[5] D. K. Spence, S. M. Wright, Concepts in Magnetic Resonance Part B, Vol. 18B(1) 15-23 (2003).
[6] E. M. Haacke et al., Magnetic Resonance Imaging-Physical principles and Sequence Design, Wiley&Sons 1999.